

Numerical observation of Hawking radiation from acoustic black holes in atomic BECs

Iacopo Carusotto,¹ Serena Fagnocchi,^{2,3} Alessio Recati,¹ Roberto Balbinot,³ and Alessandro Fabbri⁴

¹*CNR-INFM BEC Center and Dipartimento di Fisica,
Università di Trento, via Sommarive 14, I-38050 Povo, Trento, Italy**

²*Centro Studi e Ricerche “Enrico Fermi”, Compendio Viminale, 00184 Roma, Italy*

³*Dipartimento di Fisica dell’Università di Bologna and INFN sezione di Bologna, Via Irnerio 46, 40126 Bologna, Italy*

⁴*Departamento de Física Teórica and IFIC, Universidad de Valencia-CSIC, C. Dr. Moliner, 50, 46100 Burjassot, Spain*

(Dated: February 10, 2022)

We report numerical evidence of Hawking emission of Bogoliubov phonons from a sonic horizon in a flowing one-dimensional atomic Bose-Einstein condensate. The presence of Hawking radiation is revealed from peculiar long-range patterns in the density-density correlation function of the gas. Quantitative agreement between our fully microscopic calculations and the prediction of analog models is obtained in the hydrodynamic limit. New features are predicted and the effect of a finite initial temperature discussed.

Back in 1974 S. W. Hawking^{1,2} showed that black holes are not “black” but rather emit thermal radiation. This amazing prediction, crucial to establish the connection between black holes and thermodynamics³, represents a genuine quantum effect in a gravitational context and is widely considered as a milestone of modern theoretical physics. Despite its importance, the weakness of Hawking radiation has so far prevented any experimental observation. In 1981 W.G. Unruh⁴, on the basis of a formal analogy between wave motions in inhomogeneous media and quantum fields on a curved space⁵, predicted the existence of Hawking radiation in any system developing a horizon for some wavy perturbation⁶. Among the many systems that have been then proposed in this respect^{7,8}, we shall consider here the specific case of Bogoliubov phonons in an atomic Bose-Einstein condensate flowing along a one-dimensional waveguide, i.e an atom laser beam^{9,10}. Using the above analogy, a recent work¹¹ has anticipated that the presence of Hawking radiation in this setting can be unambiguously revealed from a very peculiar feature of the correlation function of density fluctuations. Here we report numerical experiments that nicely confirm this prediction. Differently from most previous works on analog models⁶, our calculations are based on the application of microscopic many-body techniques to an experimentally realistic system and never involve concepts of gravitational physics. In this way, our observations can be considered as a first independent proof of the existence of Hawking radiation and rule out the frequent concerns on the role of short wavelength, “trans-Planckian” physics on the Hawking emission¹².

Bose-Einstein condensates (BEC) of ultracold atoms are among the cleanest system where quantum physics can be investigated: the temperature is in fact so low that the behaviour of matter is dominated by the dual particle-wave nature of its constituents. Differently from other quantum coherent condensed-matter systems such as superfluid liquid Helium⁶, quantitative theories able to describe the collective dynamics from a microscopic standpoint are available: this makes ultracold atomic clouds and BECs an ideal system where to test and apply a variety of quantum theories, from many-body

physics¹³, to quantum information processing¹⁴, to the quantum field theory in curved space-times under investigation here^{6,15,16,17,18}.

The system we consider is sketched in Fig.1(a): an elongated atomic Bose-Einstein condensate which is steadily flowing at a speed v_0 along an atomic waveguide. The transverse confinement is assumed to be tight enough for the transverse degrees of freedom to be frozen¹⁹. The one-dimensional atomic density is uniform and equal to n ; the external potential $V(x)$ and the (repulsive) atom-atom interaction constant $g(x)$ are initially uniform in space and equal to respectively V_1 and g_1 .

At the time $t = 0$, a steplike spatial modulation of characteristic thickness σ_x is applied to both the potential and the interaction constant. V and g in the downstream $x > 0$ region are brought to V_2 and g_2 within a time σ_t . In an actual experiment, both the external potential and the effective atom-atom interaction constant can in fact be controlled by the transverse trapping geometry^{18,20}. The latter can also be modulated by means of a static magnetic field tuned in the vicinity of a Feshbach resonance¹⁹.

In order to suppress competing processes such as back-scattering of condensate atoms and soliton shedding from the potential step⁹, the external potential is chosen to exactly compensate the spatial jump in the interaction energy $\mu_{1,2} = g_{1,2} n$, i.e. $V_2 + \mu_2 = V_1 + \mu_1$: in this way, the condensate is able to flow undisturbed while keeping a uniform and constant average density n .

In what follows we will focus on the case when the speed of sound $c_{1,2} = \sqrt{\mu_{1,2}/m}$ in the different regions satisfies the chain inequality $c_1 > v_0 > c_2$: a sonic horizon of black hole type separates a region of subsonic $c_1 > v_0$ flow outside the black hole from a supersonic $v_0 > c_2$ one inside the black hole. As shown in Fig.1(c), long-wavelength phonon excitations in the supersonic region are dragged away by the moving condensate and are unable to propagate back to the horizon. Only higher- k , single-particle excitations outside the hydrodynamical window can emerge. In agreement with previous work²¹, dynamical stability of this black hole configuration has been verified.

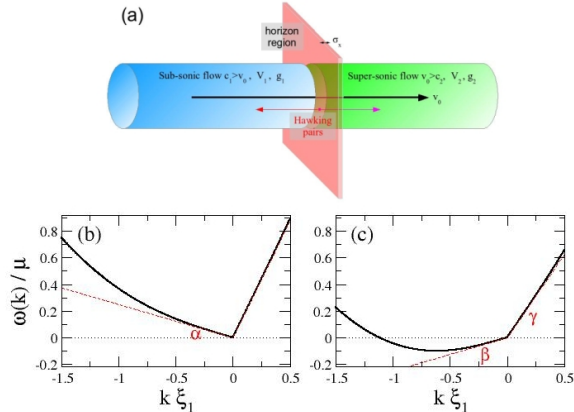


FIG. 1: Panel (a): scheme of the physical system under investigation. Panels (b,c): dispersion of Bogoliubov excitations on top of the flowing condensate in the regions of respectively sub- (b) and super-sonic (c) flow. System parameters: $c_2/c_1 = 0.5$, $v_0/c_1 = 0.75$.

The dynamics of the system following the formation of the horizon has been numerically studied by means of the so-called truncated Wigner method for the interacting Bose field. Use of this technique to calculate the time-evolution of generic observables of interacting atomic gases was recently proposed and validated²²: for dilute gases such that $n\xi \gg 1$ (the healing length being defined as usual as $\xi = \sqrt{\hbar^2/m\mu}$), this method is equivalent to the more standard Bogoliubov approach. A brief outlook of the method is given in the Methods section.

The recent advances in the experimental techniques have led to the possibility of inferring physical information on atomic gases from the correlation properties of the observed experimental noise^{23,24,25}. As the Hawking effect basically consists of the correlated emission of pairs of quanta from the region around the horizon, calculations based on the gravitational analogy¹¹ have shown that a peculiar pattern should appear in the correlation function for the density fluctuations of the condensate. Its qualitatively unique properties suggest that it should be easily distinguished from fluctuations of different, e.g. thermal origin.

In order to discard effects due to the back-action of fluctuations on the condensate wavefunction we consider the normalized, normal-order density-density correlation function

$$G^{(2)}(x, x') = \frac{\langle : n(x) n(x') : \rangle}{\langle n(x) \rangle \langle n(x') \rangle} \quad (1)$$

A snapshot of $G^{(2)}(x, x')$ at a time $t \gg \sigma_t$ well after the horizon formation is shown in Fig.2. The main features visible in the figure can be classified as follows:

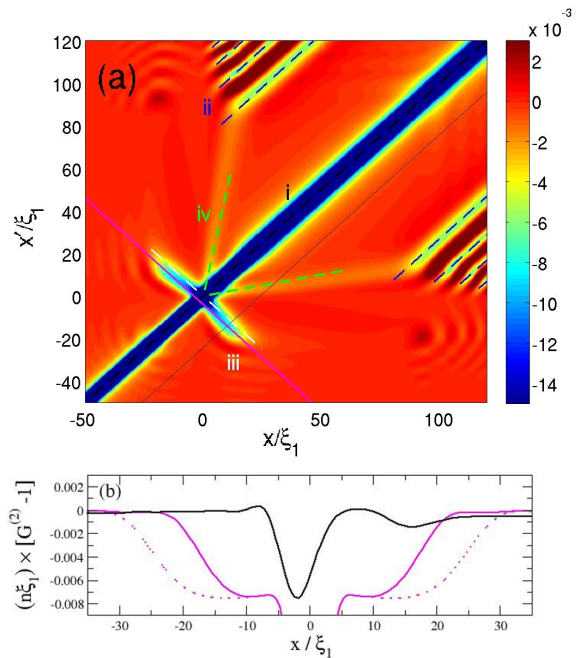


FIG. 2: Panel (a): Density plot of the universal reduced density correlation $(n\xi_1) \times [G^{(2)}(x, x') - 1]$ at a time $\mu_1 t = 70$ well after the switch-on of the horizon. The dashed lines identify the main features discussed in the text. The black and magenta lines indicate the directions along which the cuts shown in panel (b) as solid lines are taken. The dotted line in (b) corresponds to a later time $\mu_1 t = 100$. Initial temperature $T = 0$. The perturbation creating the horizon is switched on in a time $\mu_1 \sigma_t = 0.5$ and has a spatial width $\sigma_x/\xi_1 = 0.5$. Although these values were chosen to maximize the signal intensity, note that none of the qualitative features actually depends on the specific choice made. System parameters as in Fig.1.

- (i) A strong, negative correlation strip along $x = x'$ is always present.
- (ii) A system of fringes parallel to the main diagonal (blue lines) appears inside the black hole after the horizon is formed. As time goes on, the fringes move away from the $x = x'$ line at an approximately constant speed.
- (iii) Symmetric pairs of negative correlation tongues extend from the horizon point almost orthogonally to the main diagonal. While their maximum height is constant in time, their length linearly grows with time [see the cuts in panel (b)].
- (iv) Another pair of symmetric tongues appears for pairs of points located inside the black hole. Both

their height and length scale in the same way as for feature (iii).

Apart from feature (i) which is the usual antibunching due to the repulsive atom-atom interactions²⁶, these observations are a clear illustration of quantum field effects in a spatially and temporally varying background⁵.

Feature (ii) is a bulk effect and has no relation with the horizon: as a consequence of the time-modulation of the interaction constant g in the internal $x > 0$ region, correlated pairs of Bogoliubov phonons are emitted in opposite directions by a phonon analog of the dynamical Casimir effect^{27,28}. Correlation within the emitted pairs translate into the density correlations that are visible as a system of parallel fringes in the $x, x' \gg 0$ region. This identification is supported by the observation that an identical pattern is obtained for a spatially uniform system whose interaction constant is varied in time from g_1 to g_2 according to the same functional law. As usual, the longer the ramp time σ_t , the weaker the dynamical Casimir signal.

On the other hand, features (iii) and (iv) do not depend on σ_t , but rather on the eventual presence of an horizon and remain visible for indefinite time after the formation of the horizon. On the other hand, they both completely disappear if a spatially uniform system is considered or if the flow remains everywhere sub-sonic $v_0 < c_{1,2}$. This suggests a strict link to the Hawking effect

Their shape in the (x, x') correlation plane confirms this claim. As anticipated in Ref.11, the quantum correlations within a pair of Hawking phonons emitted in respectively the inward and outward direction translate into a density correlation for distant points located on either side of the horizon. Correlated Hawking phonons emitted at a generic time $t > 0$ on the α, β phonon branches of Fig.1(b,c) propagate from the horizon in respectively the outward and inward direction at speeds $v_0 - c_1 < 0$ and $v_0 - c_2 > 0$. A generic time τ after their emission they are located at $x = (v_0 - c_1)\tau$ and $x' = (v_0 - c_2)\tau$. This defines a straight line of slope $(v_0 - c_1)/(v_0 - c_2) \simeq -1$ (white dashed line), which indeed well agrees with the axis of the tongue (iii).

Feature (iv) originates from the (partial) elastic backscattering of the α Hawking partner onto branch γ . Both γ, β phonons eventually propagate in the inward direction at speeds $v_0 \pm c_2$. Again, the analytical prediction $(v_0 - c_2)/(v_0 + c_2) \simeq 1/5$ (green dashed lines) well agrees with the observed slope of the tongue.

The identification of features (iii) and (iv) as signatures of Hawking radiation is further confirmed by a quantitative comparison of our numerical data with the predictions¹¹ of the gravitational analogy (see the Methods section for the technical details). In Fig.3(a), the peak intensity of the correlation signal (iii) is plotted as a function of the inverse of the horizon region thickness σ_x , a quantity that in the gravitational analogy is proportional to the so-called surface gravity. The quantitative agreement is excellent in the limit $\sigma_x/\xi_{1,2} \gg 1$ where the physics of the many-body system is dominated by

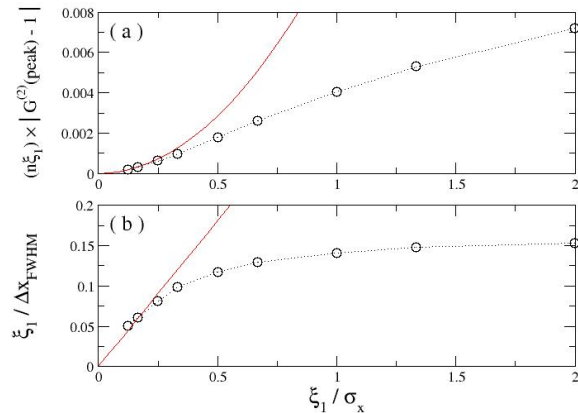


FIG. 3: Normalized peak correlation intensity (a) and inverse FWHM (b) of the correlation line as a function of the surface gravity of the horizon. Circles: numerical results. Solid lines: prediction of the gravitational analogy. Numerical uncertainty is of the order of the symbol size. Same system parameters as in Fig.1.

the hydrodynamic modes considered in the gravitational analogy. The opposite regime $\sigma_x/\xi_{1,2} \lesssim 1$ is however the most favourable to maximize the correlation signal.

The plotted quantity $(n\xi_1) \times [G^{(2)}(x, x') - 1]$ being universal within Bogoliubov theory, the actual intensity of the Hawking signal is inversely proportional to the dilution parameter $n\xi_1$: choosing a relatively strongly interacting system can therefore be favourable to maximize the signal. Although a more sophisticated theoretical approach may be required to obtain quantitative predictions in the strongly interacting $n\xi_1 \gtrsim 1$ case, the qualitative features of Hawking physics should not dramatically change.

The inverse full width at half maximum (FWHM) of the tongue (iii) in the transverse direction is plotted in Fig.3(b) as a function of the inverse thickness of the horizon region. Again, the agreement of the numerical result with the prediction of the gravitational analogy neglecting backscattering¹¹ is very good as long as $\sigma_x/\xi_1 \gg 1$. This observation appears even more significant if one remembers that the inverse FWHM is in this limit inversely proportional¹¹ to the Hawking temperature T_H .

The robustness of our observations with respect to a non-zero initial temperature is verified in Fig.4. Even for initial temperatures $k_B T/\mu_1 = 0.1$ higher than the Hawking temperature $k_B T_H/\mu_1 \simeq 0.05$ expected from the gravitational analogy⁶, the only differences with respect to Fig.2(a) consist of feature (iv) being strengthened by stimulation effects³⁰ and the appearance of an additional, well distinct tongue (v) between (iii) and (iv) due to partial reflection of thermal phonons on the horizon.

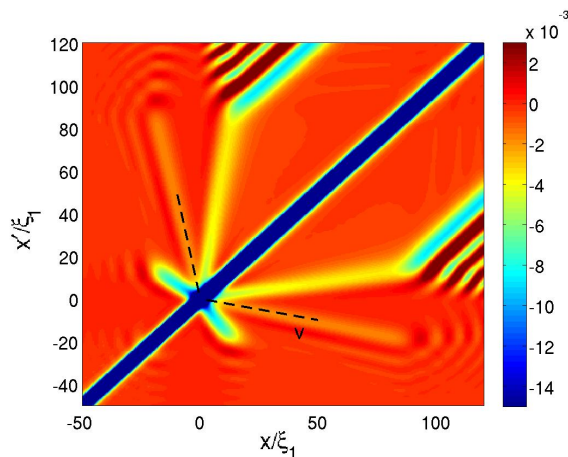


FIG. 4: Density plot of the reduced density correlation $(n\xi_1) \times [G^{(2)}(x, x') - 1]$ for the same system as in Fig.2 but for the finite initial temperature $T/\mu_1 = 0.1$.

In conclusion, we have reported numerical observation of Hawking radiation from an acoustic black hole created in a flowing Bose-Einstein condensate. The intensity of the observed signal is in quantitative agreement with the predictions of the analogy and is promising in view of forthcoming experiments. The novelty of this work consists in that all numerical results are obtained based on an *ab initio* description of the system dynamics using standard methods of microscopic many-body theory, the gravitational analogy having provided a fundamental physical insight to interpret the numerical observations. Clear evidence is reported that Hawking radiation persists even outside the hydrodynamical regime when the gravitational analogy can no longer be applied.

Acknowledgements

IC and AR are indebted to C. Lobo, Y. Castin, N. Pavloff, and Z. Gaburro for stimulating discussions. IC and AR acknowledge support from the italian MIUR. IC acknowledges support from the french CNRS. SF acknowledges support from E. Fermi center. AF acknowledges the spanish MEC.

Methods

Numerical calculations have been performed using the truncated Wigner method for interacting Bose gases. We

refer to the review paper²² for technical details.

At a time $t = t_0 \ll 0$ much before the horizon formation, the uniform ($g(x) = g_1$, $V(x) = V_1$) condensate is at thermal equilibrium at a temperature T_0 in the moving frame at v_0 . Within the Wigner framework, this corresponds to taking a random initial wavefunction $\psi_0(x)$:

$$\psi_0(x) = e^{i(k_0x - \omega_0t)} \left\{ \sqrt{n_0} + \sum_{k \neq 0} [\alpha_k u_k e^{ikx} + \alpha_k^* v_k e^{-ikx}] \right\}. \quad (2)$$

The Bogoliubov coefficients u_k, v_k are defined as $u_k \pm v_k = (E_k/\epsilon_k)^{\pm 1/4}$ in terms of the kinetic and Bogoliubov energies $E_k = \hbar^2 k^2 / 2m$ and $\epsilon_k = \sqrt{E_k(E_k + 2g_1 n)}$. The amplitudes α_k are Gaussian random variables with $\langle \alpha_k \rangle = \langle \alpha_k^2 \rangle = 0$, while the variance $\langle |\alpha_k|^2 \rangle = [2 \tanh(\epsilon_k / 2 k_B T)]^{-1}$ keeps a finite value $1/2$ even at $T = 0$ so to include zero-point fluctuations. For each realization of the random amplitudes α_k 's, the condensate density n_0 has to be suitably renormalized so to account for the condensate depletion.

The random classical wavefunction $\psi(x, t)$ is then propagated in time according to the standard Gross-Pitaevskii equation (GPE): $i\hbar \partial_t \psi = -(\hbar^2/2m) \partial_x^2 \psi + V(x, t) \psi + g(x, t) |\psi|^2 \psi$ starting from $\psi_0(x)$. Expectation values of symmetrically-ordered field observables at any later time t are obtained as the corresponding averages of the classical field over the random initial condition ψ_0 . Periodic boundary conditions are assumed, but an absorbing region far from the horizon is required to prevent spurious dynamical instabilities due to excitations circulating around the integration box^{21,29}.

The external potential and the atom-atom interaction constant have the form $V(x, t) = V_1 + (V_2 - V_1) \tilde{\Theta}(x/\sigma_x) \tilde{\Theta}(t/\sigma_t)$ and $g(x, t) = g_1 + (g_2 - g_1) \tilde{\Theta}(x/\sigma_x) \tilde{\Theta}(t/\sigma_t)$. The generalized Θ -function $\tilde{\Theta}(z)$ smoothens the usual $\Theta(z)$ step function on a scale $\Delta z \simeq 1$. Having $V_1 + ng_1 = V_2 + ng_2$ guarantees that the plane wave $\psi(x, t) = \sqrt{n} \exp[i(k_0x - \omega_0t)]$ is a solution of the GPE for all times¹⁹.

The peak value of the correlation signal and the FWHM have been extracted from a cut of $G^{(2)}(x, x')$ along a straight line $x = x' + x_{cut}$ well outside the many-body dip [the black line in Fig.2(a)]. Note that the minimum value of $G^{(2)}$ along this cut almost does not depend on its exact position x_{cut} nor the observation time.

- * Electronic address: carusott@science.unitn.it
- ¹ S. W. Hawking, *Black hole explosions?*, Nature (London) **248**, 30 (1974).
 - ² S. W. Hawking, *Particle creation by black holes*, Commun. Math. Phys. **43**, 199 (1975).
 - ³ J. D. Bekenstein, *Black Holes and Entropy*, Phys. Rev. D **7**, 2333 (1973).
 - ⁴ W.G. Unruh, *Experimental Black-Hole Evaporation?*, Phys. Rev. Lett. **46**, 1351 (1981).
 - ⁵ N. D. Birrell and P. C. W. Davies, *Quantum fields in curved space* (Cambridge University Press, Cambridge, UK, 1982).
 - ⁶ *Artificial Black Holes*, edited by M. Novello, M. Visser, and G. Volovik (World Scientific, River Edge, 2002).
 - ⁷ U. Leonhardt and P. Piwnicki, *Relativistic effects of light in moving media with extremely low group velocity*, Phys. Rev. Lett. **84**, 822 (2000).
 - ⁸ R. Schützhold and W. G. Unruh, *Hawking Radiation in an Electromagnetic Waveguide?*, Phys. Rev. Lett. **95**, 031301 (2005).
 - ⁹ N. Pavloff, *Breakdown of superfluidity of an atom laser past an obstacle*, Phys. Rev. A **66**, 013610 (2002).
 - ¹⁰ W. Guerin, J.-F. Riou, J. P. Gaebler, V. Josse, P. Bouyer, and A. Aspect, *Guided Quasicontinuous Atom Laser*, Phys. Rev. Lett. **97**, 200402 (2006).
 - ¹¹ R. Balbinot, A. Fabbri, S. Fagnocchi, *Non-local density correlations as signal of Hawking radiation in BEC acoustic black holes*, preprint arXiv:0711.4520.
 - ¹² T. Jacobson, *Black-hole evaporation and ultrashort distances*, Phys. Rev. D **44**, 1731 (1991).
 - ¹³ I. Bloch, J. Dalibard, W. Zwerger, *Many-Body Physics with Ultracold Gases*, accepted for publication in Rev. Mod. Phys. (2008).
 - ¹⁴ J. J. García-Ripoll, P. Zoller, and J.I. Cirac, *Quantum information processing with cold atoms and trapped ions*, J. Phys. B: At. Mol. Opt. Phys. **38** S567 (2005).
 - ¹⁵ L. J. Garay, J. R. Anglin, J. I. Cirac, and P. Zoller, *Sonic analog of gravitational black holes in Bose-Einstein condensates*, Phys. Rev. Lett. **85**, 4643 (2000).
 - ¹⁶ C. Barceló, S. Liberati, and M. Visser, *Towards the observation of Hawking radiation in Bose-Einstein condensates*, Int. J. Mod. Phys. **A18** 3735 (2003).
 - ¹⁷ P. O. Fedichev and U. R. Fischer, *Gibbons-Hawking effect in the sonic de Sitter space-time of an expanding Bose-Einstein-condensed gas*, Phys. Rev. Lett. **91**, 240407 (2003).
 - ¹⁸ C. Barceló, S. Liberati, and M. Visser, *Probing semiclassical analog gravity in Bose-Einstein condensates with widely tunable interactions*, Phys. Rev. A **68**, 053613 (2003).
 - ¹⁹ L. Pitaevskii and S. Stringari, *Bose-Einstein condensation* (Clarendon Press, Oxford, 2003).
 - ²⁰ M. Olshanii, *Atomic Scattering in the Presence of an External Confinement and a Gas of Impenetrable Bosons*, Phys. Rev. Lett. **81**, 938 (1998).
 - ²¹ C. Barceló, A. Cano, L. J. Garay, and G. Jannes, *Stability analysis of sonic horizons in Bose-Einstein condensates*, Phys. Rev. D **74**, 024008 (2006).
 - ²² A. Sinatra, C. Lobo, Y. Castin, *The truncated Wigner method for Bose condensed gases: limits of validity and applications*, J. Phys. B **35**, 3599 (2002).
 - ²³ M. Greiner, C. A. Regal, J. T. Stewart, and D. S. Jin, *Probing Pair-Correlated Fermionic Atoms through Correlations in Atom Shot Noise*, Phys. Rev. Lett. **94**, 110401 (2005).
 - ²⁴ S. Fölling, F. Gerbier, A. Widera, O. Mandel, T. Gericke, I. Bloch, *Spatial quantum noise interferometry in expanding ultracold atom clouds*, Nature **434**, 481 (2005).
 - ²⁵ A. Perrin, H. Chang, V. Krachmalnicoff, M. Schellekens, D. Boiron, A. Aspect, and C. I. Westbrook, *Observation of Atom Pairs in Spontaneous Four-Wave Mixing of Two Colliding Bose-Einstein Condensates*, Phys. Rev. Lett. **99**, 150405 (2007).
 - ²⁶ M. Naraschewski and R. J. Glauber, *Spatial coherence and density correlations of trapped Bose gases*, Phys. Rev. A **59**, 4595 (1999).
 - ²⁷ K. Staliunas, S. Longhi, and G. J. de Valcárcel, *Faraday Patterns in Bose-Einstein Condensates*, Phys. Rev. Lett. **89**, 210406 (2002).
 - ²⁸ M. Krämer, C. Tozzo, and F. Dalfovo, *Stability diagram and growth rate of parametric resonances in Bose-Einstein condensates in one-dimensional optical lattices*, Phys. Rev. A **71**, 061602(R) (2005).
 - ²⁹ S. Corley and T. Jacobson, *Black hole lasers*, Phys. Rev. D **59**, 124011 (1999).
 - ³⁰ J. D. Bekenstein and A. Meisels, *Einstein A and B coefficients for a black hole*, Phys. Rev. D **15**, 2775 (1977).